A population pharmacokinetic model of AT9283 in adults and children to predict the maximum tolerated dose in children with leukaemia

Janna K Duong[1], Melanie J Griffin[2], Darren Hargrave[3], Josef Vormoor[2], David Edwards[4], Alan V Boddy[1].[1]Faculty of Pharmacy, The University of Sydney, Sydney, Australia; [2]Northern Institute for Cancer Research, Newcastle, United Kingdom; [3]Great Ormond Street Hospital for Children NHS Foundation Trust, London, United Kingdom; [4]Cancer Research UK, London, United Kingdom.

Running title: AT9283 pharmacokinetics in adults and children

Words: 2,891 words

Figures: 4

Tables: 4

Keywords: aurora kinase inhibitor, pharmacokinetics, adults, pediatric, solid tumour, hematological disease, maximum tolerated dose, Phase I oncology trial.

Corresponding author

Dr Janna K Duong

Faculty of Pharmacy, Pharmacy and Bank Building A15, The University of Sydney, Email: janna.duong@sydney.edu.au

SUMMARY

Aims AT9283 is used to treat patients with solid tumors and patients with leukaemia. However, the maximum tolerated dose (MTD) for children with leukaemia remains unknown due to early termination of the Phase I trial. The aim of this study was to develop a population model of AT9283 to describe the pharmacokinetics in adults and children and to estimate the MTD in children with leukaemia.

Methods Data from Phase I dose-escalation studies in adults and children were used to build a population pharmacokinetic model (NONMEM v7.3). Potential covariates investigated included body weight, body surface area (BSA), glomerular filtration rate (GFR), age and sex. Model-derived AUC was used to investigate the relationship between dose and exposure in adults and children.

Results The plasma concentrations of AT9283 (n = 1770) from 92 patients (53 adults, 39 children) were used to build a two-compartment model with all pharmacokinetic parameters scaled using body weight. Renal function (GFR), but not BSA, was a significant covariate for the clearance of AT9283. In children with leukaemia (median weight 16 kg), a flat dose of 500 mg/72 h provided similar drug exposures at the MTD as the adult population. The estimated MTD for children with leukaemia, therefore, is 30 mg/kg/72 h.

Conclusion For adults, GFR was a significant predictor of CL, whilst body-weight based dosing was more useful than BSA in determining the drug exposure in children. The MTD was estimated to be 30 mg/kg/72 h children with leukaemia.

WHAT IS ALREADY KNOWN ABOUT THIS SUBJECT

- Adults with leukaemia can tolerate a 10-fold higher dose of AT9283 than adults with solid tumors.
- AT9283 is dosed by body surface area (BSA) but other factors influencing the pharmacokinetics of AT9283 were not investigated
- The maximum tolerated dose (MTD) of AT9283 in children with leukaemia is not known.

WHAT THIS STUDY ADDS

- A population pharmacokinetic model was used to combine the adult and children studies to investigate factors that may influence the pharmacokinetics of AT9283.
- GFR and body weight are better predictors of clearance than BSA
- Doses of 30 mg/kg/72h in children with leukaemia would provide similar exposure levels to that seen in adults with leukaemia at the maximum tolerated doses (MTD).

1. INTRODUCTION

The Aurora kinases (A, B and C) play a critical role in the cell mitotic process [1, 2]. Aurora Kinase A is involved in centrosome function, mitotic entry and spindle assembly, whilst Aurora Kinase B is a chromosomal passenger protein and is involved in chromatin modification, microtubule-kinetochore attachment, spindle checkpoint and cytokinesis [1, 3]. Aurora Kinase C is also a chromosomal passenger protein, and exhibits similar functions to Aurora Kinase B [3]. Aurora kinases are overexpressed in many cancers, therefore aurora kinase inhibitors are promising anticancer drugs. Aurora kinase inhibitors may be particularly useful against hematologic malignancies due to greater genetic homogeneity and greater proliferations rates relative to solid tumours [4, 5].

AT9283 (Astex Pharmaceuticals®) is a multi-targeted aurora kinase inhibitor found to be a potent inhibitor of Aurora A, Aurora B and other kinases including JAK2, FLT3 and Abl (T315I) [6]. In adults and children with solid tumours, AT9283 demonstrated significant aurora kinase inhibition at tolerable doses with disease stabilization [4, 7]. However, the use of AT9283 is limited by its toxicity profile. Some of these dose-limiting toxicities (DLTs) included neutropenia (grade 3-4), tumor lysis syndrome, bacterial infections cardiovascular and gastrointestinal disorders [4, 7, 8].

AT9283 is administered as a continuous 72-hour infusion and is dosed by body surface area (BSA). In Phase I studies of AT9283, the maximum tolerated dose (MTD) was identified for adults with solid tumors (27 mg/m^2/72h) [7], adults with leukaemia (324 mg/m^2/72h) [8] and for children with solid tumors (55.5 mg/m^2/72h) [4]. The Phase I study for children with

leukaemia, however, was terminated due to a slow recruitment rate. Only seven children were recruited in this study and the maximum dose level reached was 69 mg/m^2/72h.

The pharmacokinetics of AT9283 was previously investigated using a non-compartmental approach in each population group [4, 7, 8]. Each pharmacokinetic study noted large inter-individual variability (IIV) in the pharmacokinetics of AT9283, even after adjusting doses for BSA [4]. Furthermore, the increase in exposure to AT9283 was proportional to absolute administered dose, rather than the BSA-based dosing level [4]. A better understanding of the relationship between AT9283 doses and plasma concentration, as well as determinants of drug exposure, will enable doses of AT9283 to be optimized for each patient population.

Population pharmacokinetic modelling and simulation is an industry standard method of investigating the pharmacokinetics of a drug to identify measurable pathophysiological factors influencing the pharmacokinetics of the drug [9]. In this study, the data from adult and children studies were pooled to describe the pharmacokinetics in these population groups. Furthermore, this population model was used to simulate doses in children with leukaemia and to estimate what the MTD would be in this population.

2. METHODS

2.1 Datasets and study design

Phase I data for this investigation originated from four separate pharmacokinetic studies in adults ([7, 8]; NCT00443976, NCT00522990) and children ([4]; NCT0098568, NCT01431664) and were sponsored by Astex Pharmaceuticals and Cancer Research UK., respectively. These dose-

escalation studies were designed to investigate the safety and tolerability of AT9283 in each population group and to establish a dose for Phase II studies (Table 1). The conventional 3 + 3 study design was used for the adults (solid tumor and leukaemia) and children with leukaemia, whilst the rolling six design was used for children with solid tumors.

Written informed consent was obtained from all patients and from all parents and guardians of children. These studies were approved by the local ethics committees for each trial centre (various locations in the U.S. and the U. K.) [4, 7, 8, 10] and were conducted to Good Clinical Practice in accordance with the Declaration of Helsinki and its amendments.

2.2 AT9283 dosing

AT9283 was administered as a continuous three-day (72 h) i.v. infusion every 21 days via central venous access. The doses of AT9283 were adjusted according to body surface area (BSA), which was calculated using the Mosteller formula [11]. The maximum tolerated dose (MTD) was defined as the highest dose that could be given based on the incidence of dose-limiting toxicities (DLTs). For the 3 + 3 design, the MTD was defined as the dose given to three patients with less than one patient experiencing a DLT. For the rolling six design, the MTD is the dose given to six patients with less than one patient experiencing a DLT.

2.3 AT9283 concentrations

Blood samples for pharmacokinetic analyses were collected during the first and second cycle for the adult studies and during the first cycle for studies conducted in children. The time-points for blood collection are outlined in Table 1. The concentrations of AT9283 were quantified using a

validated LC-MS/MS assay [4] (Astex Investigator's Brochure) over a calibration range of 0.1 – 500 ng/mL. The lower limit of quantification (LLOQ) was 0.1 ng/mL.

2.4 Population modelling

Population pharmacokinetic analyses were conducted using the population modelling package NONMEM® 7.3.0 (ICON Development Solutions, Hanover, MD, USA) [12] with first-order conditional estimation method with interaction (FOCE-I). Model development was managed using Perl-Speaks-NONMEM 3.5.3 [13], Pirana 2.8.1[14] and R (Version 3.2.5) [15]. Model selection was informed by using the objective function value (OFV, -2log likelihood) [16], whereby a reduction of ≥3.84 points in OFV was considered statistically significant (P <0.05 with d.f. = 1, approximate asymptotic x^2-distribution).

2.4.1 Structural and statistical model

The pharmacokinetics of AT9283 was tested using one-compartment and two-compartment structural models. The inter-individual variability (IIV) is the unexplained random variability between individuals, which was described using a log-normal distribution (Eq. 1):

$$P_i = P_{TV} \times exp^{(n_i)} \quad (1)$$

where P_i is the pharmacokinetic parameter of the i^{th} individual. P_{TV} is the typical population parameter value, n_i is the IIV in the i^{th} individual with a distribution of $N(0, \omega_{IIV}^2)$.

Different error models were tested to describe the residual unexplained variability of the data (additive, proportional, mixed, exponential, log-transformation). A separate residual error model was also evaluated for each of the studies to account for variability in the assays. Only 3%

of the observations of the dataset were below the limit of quantification, and were therefore excluded from the analysis.

2.4.2 Covariate model

Potential covariates were evaluated by visual inspection of the empirical Bayes estimates (EBEs) against the covariates and by step-wise inclusion into the model. The covariates investigated included measurements of body size (body weight, BMI, lean body weight, BSA, fat-free mass [17]), cancer type and kidney function (glomerular filtration rate, GFR). The backward elimination of covariates was used to confirm covariate selection, whereby an increase in OFV (>6.63, P <0.01) was required.

For continuous covariates, linear, piecewise-linear, exponential and power relationships were investigated. There were only two children aged under 2 years, therefore a model to describe CL maturation with age for children under 2 years was not needed.

An allometric weight model was used to standardize all pharmacokinetic parameters to a body weight of 70 kg [18]. The allometric weight model for the clearance parameters and volume parameters are shown in Eq. 2 and 3, respectively.

$$F_{CL} = \left(\frac{WT}{WT_{STD}}\right)^{0.75} \quad (2)$$

$$F_{V} = \left(\frac{WT}{WT_{STD}}\right)^{1} \quad (3)$$

Where a standard weight value of 70 kg (WT_{STD}) was used to normalize pharmacokinetic parameters in adults and children.

For adults, GFR was estimated using the Modification of Diet in Renal Disease (MDRD) formula for adults [19] (Eq. 4):

$$GFR\ (mL/min/1.73m^2) = 175 \times [serum\ creatinine\ (\mu mol/L)]^{-1.154} \times Age\ (years)^{-0.203} \times k \quad (4)$$

where k is 1 for males and 0.742 for females.

For children aged under 18 years, the bedside Schwartz formula [20] was used (Eq. 5):

$$GFR\ (mL/min/1.73m^2) = \frac{41.3\ x\ height\ (cm)}{serum\ creatinine\ (\mu mol/L) \times 0.01131} \quad (5)$$

2.4.3 Model evaluation

The model was evaluated by visual inspection of goodness of fit plots of the observed and predicted concentrations and conditional weighted residuals (CWRES). The final model performance was examined by using prediction-corrected visual predictive checks (VPCs) to compare the 5th, 50th and 95th percentiles of the observed concentrations and simulations of concentration–time profiles (1,000 replicates) from the final model [21]. A nonparametric bootstrap method [22] (n = 1,000) was used to study the uncertainty of all pharmacokinetic parameter estimates in the final model to obtain the median and 95% confidence interval of the parameter estimates. Significant differences between baseline measurements were evaluated using the unpaired *t* test in R. A *P* value of <0.05 was considered statistically significant.

2.5 AT9283 exposure

The final model was used to calculate the area-under the curve ($AUC_{0-\infty}$) of AT9283 using post-hoc estimates of CL ($AUC_{0-\infty}$ = Dose/CL). Using the final model, stochastic simulations were performed to simulate concentration-time profiles (n = 1,000) using the median dose and median BSA for patients who were administered the MTD dose. The concentrations of AT9283 at the

MTD were compared to investigate the variability in the drug exposure for the different patient groups.

For children with leukaemia, dosing simulations were conducted to target a similar range of $AUC_{0-\infty}$ to that seen in adults with leukaemia. Since there were limited data for children with leukaemia, the exposure-toxicity relationship was assumed to be the same in adults and children.

3. Results

3.1 Study population

A summary of the patient demographics is shown in Table 2. The dose administered ranged from 4.5 mg/m^2/72 h to 486 mg/m^2/72h. For children with leukaemia, the trial was terminated at a dose of 69 mg/m^2/72 h. About half of the adult population had mild to moderately reduced kidney function (GFR <90 mL/min/1.73m^2), whilst children had predominately healthy kidney function (GFR > 100 mL/min/1.73m^2) (Table 2, Supplementary Figure 1). Compared to children (GFR, 132.9 [47.4 – 299.4] mL/min/1.73m^2, median [range]), most adults had some form of kidney dysfunction (GFR, 77.1 [31.9 – 170.5] mL/min/1.73m^2; P <0.001). As expected, there was larger variability in the BSA in children than in adults. Children with leukaemia were younger (difference between the medians of 7 years, P <0.01) and had a smaller BSA (0.34 m^2, P <0.001), compared to children with solid tumors.

3.2 Population model

A total of 1770 observations from 92 individuals were used for population analyses. This dataset was best described using a two-compartment model. All observations were log-transformed and the residual variability was described using a combined additive and proportional error model for the adult population and an additive error model for children. The separate error model for the adults and children was used to account for site-specific variability in sample collection and the analytical assays (ΔOFV -118.1). The IIV was estimated on all parameters. The correlations between the IIV of each parameter was estimated using a full covariance matrix.

The influence of body size on the pharmacokinetic parameters for adults and children was best described using an allometric model with body weight for CL. An empirical GFR power model was used to describe the effect of renal function on clearance, normalized to a standard of 6 L/h (100 mL/min), which significantly improved the model (ΔOFV -66.3, reduced IIV by 1.6%). There were no significant differences between the CL of AT9283 in patients with solid tumors (25.5 [9.0 – 66.7] L/h) and patients with leukaemia (27.8 [4.3 – 48.0] L/h, P = 0.12). Cancer type was not a significant covariate in the model for any pharmacokinetic parameter (did not reduce the IIV). The final equations for CL and V_C were (Eq. 6 and 7):

$$CL = \theta_{CL} \times \left(\frac{WT}{WT_{STD}}\right)^{0.75} \times \left(\frac{GFR}{GFR_{STD}}\right)^{\theta_{EC}} \quad (6)$$

$$V_C = \theta_{VC} \times \left(\frac{WT}{WT_{STD}}\right)^{1} \quad (7)$$

Where θ_{EC} is the estimated power parameter for GFR.

The goodness-of-fit plots showed that the final model described the pharmacokinetics of AT9283 in adults and children with no apparent bias (Figure 1). There was good agreement between the observed concentrations and model predictions for children throughout different weight categories

(Supplementary Figure 3). The VPCs revealed good agreement between the model simulations and the 5th, 50th and 95th percentiles of the observations and the model adequately described the time-course of AT9283 concentrations (Figure 2). The simulated prediction intervals for children post-infusion are wide due to the lack of data collected after 80 hours. All parameters were estimated with acceptable precision (residual standard error <30%), without any significant shrinkage (<30%) and the non-parametric bootstrap indicated that the model was robust (Table 3).

3.3 AT9283 exposure

AT9283 exposure at the MTD was investigated using the median covariate values of each population group (Table 4, Figure 3). In the solid tumor studies, the MTD was 27 mg/m^2/72h for adults and 55.5 mg/m^2/72h for children. Using the median BSA, these doses are equivalent to median doses of 51 mg/72h and 68 mg/72 h, in adults and children, respectively. The median MTD in adults with leukaemia was 10-fold higher (567 mg/72h) than for patients with solid tumours, with a median $AUC_{0-\infty}$ of 20, 956 h.ng/mL (4,774– 76,805 h.ng/mL, range). Children with leukaemia (median weight 16 kg) only reached an $AUC_{0-\infty}$ of 2,949 h.ng/mL (539 – 9,988 h.ng/mL, range) at the median maximum dose administered (51 mg/72h). To reach an MTD drug exposure comparable to that in adults with leukaemia, children with leukaemia would require doses of 500 mg/72 h, to achieve an $AUC_{0-\infty}$ of 38,254 h.ng/mL (9694 – 124,430 h.ng/mL) (Figure 3). To account for the range of weights in children, doses of 30 mg/kg/72 h would provide a more consistent exposure in children rather than a flat dose of 500 mg/72 h (Supplementary Figure 4). Figure 4 shows the differences in the drug exposure with varying GFR and weight at a dose of 30 mg/kg/72 h. A weight-based dosing regimen reduced the

variability in the drug exposure for children, whilst the effect of GFR would be significant only for patients with poor kidney function.

4. DISCUSSION

The primary objective of oncology Phase I dose-finding studies is to determine the MTD and the dose level below the MTD is usually carried forward to Phase II oncology trials [23, 24]. However, there are numerous issues that may prevent the completion of Phase I oncology trials. Firstly, the recruitment rate may be slow because only patients who are resistant to standard treatment are eligible. Secondly, Phase I oncology trials have a long dose-escalation scheme, with initial doses far below the MTD to minimize toxicity, which consequently increases the number of patients treated at sub-therapeutic doses. In the case of the AT9283 trial in children with leukaemia, the lowest target inhibitory dose was used as the starting dose due to some concerns with cardiotoxicity in the adult studies [8]. However, the combination of slow recruitment with a coincident increase in competing studies and long dose-escalation scheme eventually led to the termination of the trial. The population pharmacokinetic approach was therefore used to estimate what the MTD would be for children with leukaemia. One of the main advantages of using the population approach is that the data from adults and children can be combined to provide robust estimates of the pharmacokinetics of AT9283 (Figure 1 and 2).

The adult and child datasets were combined by adjusting all pharmacokinetic parameters for body weight. Compared to BSA, the inclusion of body weight as a covariate provided the largest drop in OFV. Body weight is also the preferred covariate for body size because it is

directly measurable and estimating BSA for small children is difficult [25]. Furthermore, renal function as estimated by GFR, was found to be a significant covariate for CL, consistent with the finding that 20-30% of the drug is eliminated in the urine [7].

The absolute MTD administered to adults and children with solid tumours were similar, after accounting for the differences in BSA. Previous studies have reported a much higher MTD for children with solid tumours (55.5 mg/m^2/72h) [4] compared to adults with solid tumors (27 mg/m^2/72h) [7], which corresponded to mean absolute doses of 67.7 mg/72 h and 51.3 mg/72h in children and adults, respectively. Children with solid tumors had an approximately 25% higher AUC compared to adults with solid tumors (Figure 3, Supplementary Figure 2). Considering that most responses occur within 80% and 120% of the MTD [23, 24, 26], the potential MTD dose range in adults with solid tumors (41 to 61.6 mg/72 h, range) is comparable to the MTD dose range in children with solid tumors (54.2 to 81.2 mg/72 h).

The main dose limiting toxicity (DLT) of AT9283 was febrile neutropaenia [7], therefore patients with leukaemia can tolerate much higher doses of AT9283. In adults with leukaemia the MTD (567 mg/72 h) resulted in a 10-fold higher drug exposure (median $AUC_{0-\infty}$: 20, 956 h.ng/mL; range, 4,774 – 76, 805 h.ng/mL) compared to adults with solid tumors (Figure 3). To achieve this same level of exposure, we estimated that the MTD would need to be 10-fold higher than the maximum dose administered to children with leukaemia. We have found that doses of 30 mg/kg/72 h are suitable for children to obtain a similar drug exposure to that see in adults with leukaemia at the MTD.

The AUC of AT9283 is higher for patients with poor kidney function and for patients with large body size (Figure 4). Since children enrolled in the Phase I studies have predominately

normal kidney function, GFR was a more relevant predictor of AT9283 exposure in adults (GFR 77.1 [31.9 – 170.5] mL/min/1.73m^2). In contrast, body weight is a more relevant predictor of drug exposure in children, particularly for children at the extremes of body weight (Figure 4).

A limitation of this study is the small sample size in children with leukaemia (n = 7). Children with leukaemia were also the youngest population group and had the smallest body size. Since there is limited data on very young children, large variability in the concentrations of AT9283 was observed in our simulations of children with leukaemia (Figure 3).

We have provided an estimate of the MTD in children with leukaemia, which is based on achieving a target AUC. However, the identified MTD in Phase I studies was based on the incidence of DLTs at discrete dosing levels. The MTD represents the dose for which the percentage experiencing the DLT ranges from 15% to 70%, which may differ significantly from the actual MTD [27]. Since Phase I oncology studies only assessed the toxicity profile of anticancer drugs, it is not known how the MTD relates to the efficacy of AT9283. Knowledge of the exposure-response relationship of AT9283 would provide a better indication of the target AUC required to achieve an optimal response.

4.1 Conclusions

The population pharmacokinetic analysis provides a method of shortening the time to reach the MTD by potentially reducing the number of patients enrolled in dose-escalation trials and the number of patients treated at sub-therapeutic doses. We have found weight to be a better predictor of the pharmacokinetics of AT9283 rather than BSA for children, whilst GFR is a

relevant predictor of CL, for adults. If the Phase I trial was to be completed in children with leukaemia, we estimated that the MTD for children with leukaemia would be 30 mg/kg/72 h, which is about 10-fold higher than the maximum dose tested.

ACKNOWLEDGEMENTS

The authors would like to thank Astex Pharmaceuticals and Cancer Research UK for the datasets used in this manuscript.

CONFLICTS OF INTEREST

David Edwards is employed by Cancer Research U. K. Darren Hargrave is supported by the National Institute for Health Research Biomedical Research Centre at Great Ormond Street Hospital for Children NHS Foundation Trust and University College London.

Reference list

1. Fu J, Bian M, Jiang Q, Zhang C. Roles of Aurora kinases in mitosis and tumorigenesis. Mol Cancer Res 2007; 5: 1-10.
2. Carmena M, Earnshaw WC. The cellular geography of aurora kinases. Nat Rev Mol Cell Biol 2003; 4: 842-54.
3. Dar AA, Goff LW, Majid S, Berlin J, El-Rifai W. Aurora kinase inhibitors--rising stars in cancer therapeutics? Mol Cancer Ther 2010; 9: 268-78.
4. Moreno L, Marshall LV, Pearson AD, Morland B, Elliott M, Campbell-Hewson Q, Makin G, Halford SE, Acton G, Ross P, Kazmi-Stokes S, Lock V, Rodriguez A, Lyons JF, Boddy AV, Griffin MJ, Yule M, Hargrave D. A phase I trial of AT9283 (a selective inhibitor of aurora kinases) in children and adolescents with solid tumors: a Cancer Research UK study. Clin Cancer Res 2015; 21: 267-73.
5. Bavetsias V, Linardopoulos S. Aurora Kinase Inhibitors: Current Status and Outlook. Front Oncol 2015; 5: 278.
6. Howard S, Berdini V, Boulstridge JA, Carr MG, Cross DM, Curry J, Devine LA, Early TR, Fazal L, Gill AL, Heathcote M, Maman S, Matthews JE, McMenamin RL, Navarro EF, O'Brien MA, O'Reilly M, Rees DC, Reule M, Tisi D, Williams G, Vinkovic M, Wyatt PG. Fragment-based discovery of the pyrazol-4-yl urea (AT9283), a multitargeted kinase inhibitor with potent aurora kinase activity. J Med Chem 2009; 52: 379-88.
7. Arkenau HT, Plummer R, Molife LR, Olmos D, Yap TA, Squires M, Lewis S, Lock V, Yule M, Lyons J, Calvert H, Judson I. A phase I dose escalation study of AT9283, a small molecule inhibitor of aurora kinases, in patients with advanced solid malignancies. Ann Oncol 2012; 23: 1307-13.
8. Foran J, Ravandi F, Wierda W, Garcia-Manero G, Verstovsek S, Kadia T, Burger J, Yule M, Langford G, Lyons J, Ayrton J, Lock V, Borthakur G, Cortes J, Kantarjian H. A phase I and pharmacodynamic study of AT9283, a small-molecule inhibitor of aurora kinases in patients with relapsed/refractory leukemia or myelofibrosis. Clin Lymphoma Myeloma Leuk 2014; 14: 223-30.
9. US FDA. Guidance for industry. Population pharmacokinetics. 2009. Available at: http://www.fda.gov/downloads/Drugs/Guidances/UCM072137.pdf. Accessed March 2016.
10. Vormoor B, Veal GJ, Griffin MJ, Boddy AV, Irving J, Minto L, Case M, Banerji U, Swales KE, Tall JR, Moore AS, Toguchi M, Acton G, Dyer K, Schwab C, Harrison CJ, Grainger JD, Lancaster D, Kearns P, Hargrave D, Vormoor J. A phase I/II trial of AT9283, a selective inhibitor of aurora kinase in children with relapsed or refractory acute leukemia: challenges to run early phase clinical trials for children with leukemia. Pediatr Blood Cancer 2016.
11. Mosteller RD. Simplified calculation of body-surface area. N Engl J Med 1987; 317: 1098.
12. Beal S, Sheiner LB, Boeckmann A, Bauer RJ. NONMEM user guides. Ellicott City, MD, USA: ICON Development Solutions, 1989 - 2011.
13. Lindbom L, Pihlgren P, Jonsson EN. PsN-Toolkit--a collection of computer intensive statistical methods for non-linear mixed effect modeling using NONMEM. Comput Methods Programs Biomed 2005; 79: 241-57.

14. Keizer RJ, van Benten M, Beijnen JH, Schellens JH, Huitema AD. Pirana and PCluster: a modeling environment and cluster infrastructure for NONMEM. Comput Methods Programs Biomed 2011; 101: 72-9.
15. R Core Team (2015). R: A language and environment for statistical computing. R Foundation for Statistical Computing, Vienna, Austria. URL http://www.R-project.org/.
16. Wang Y. Derivation of various NONMEM estimation methods. J Pharmacokinet Pharmacodyn 2007; 34: 575-93.
17. Janmahasatian S, Duffull SB, Ash S, Ward LC, Byrne NM, Green B. Quantification of lean bodyweight. Clin Pharmacokinet 2005; 44: 1051-65.
18. Anderson BJ, Holford NH. Mechanism-based concepts of size and maturity in pharmacokinetics. Annu Rev Pharmacol Toxicol 2008; 48: 303-32.
19. Levey AS, Bosch JP, Lewis JB, Greene T, Rogers N, Roth D. A more accurate method to estimate glomerular filtration rate from serum creatinine: a new prediction equation. Modification of Diet in Renal Disease Study Group. Ann Intern Med 1999; 130: 461-70.
20. Schwartz GJ, Munoz A, Schneider MF, Mak RH, Kaskel F, Warady BA, Furth SL. New equations to estimate GFR in children with CKD. J Am Soc Nephrol 2009; 20: 629-37.
21. Post TM, Freijer JI, Ploeger BA, Danhof M. Extensions to the visual predictive check to facilitate model performance evaluation. J Pharmacokinet Pharmacodyn 2008; 35: 185-202.
22. Henderson AR. The bootstrap: a technique for data-driven statistics. Using computer-intensive analyses to explore experimental data. Clin Chim Acta 2005; 359: 1-26.
23. Huson LW. Phase I oncology trials incorporating patient choice of dose. Br J Cancer 2012; 107: 1022-4.
24. Joffe S, Miller FG. Rethinking risk-benefit assessment for phase I cancer trials. J Clin Oncol 2006; 24: 2987-90.
25. Sharkey I, Boddy AV, Wallace H, Mycroft J, Hollis R, Picton S, Chemotherapy Standardisation group of the United Kingdom Children's Cancer Study G. Body surface area estimation in children using weight alone: application in paediatric oncology. Br J Cancer 2001; 85: 23-8.
26. Penel N, Duhamel A, Adenis A, Devos P, Isambert N, Clisant S, Bonneterre J. Predictors for establishing recommended phase 2 doses: analysis of 320 dose-seeking oncology phase 1 trials. Invest New Drugs 2012; 30: 653-61.
27. Faries D. Practical modifications of the continual reassessment method for phase I cancer clinical trials. J Biopharm Stat 1994; 4: 147-64.

Figure Legends

Figure 1. Goodness-of-fit plots of the final model. The open circles are the observations from the adult dataset and the open triangles are the observations from the children. The population prediction and individual prediction plots are shown with the line of identity (black) and a linear regression line (blue). Plots of CWRES are shown with a loess smooth (blue line). *CWRES*, conditional weighted residuals.

Figure 2. Prediction-corrected visual predictive checks (VPCs) of the AT9283 concentrations stratified by population. The dots are the observations plotted with the median observed AT9283 concentrations (red line) and the 5^{th} and 95^{th} percentiles of the observed concentrations (dotted blue lines). The shaded areas are the 95% confidence intervals of the 5^{th}, 50^{th} and 95^{th} percentiles of the simulated concentrations.

Figure 3. Simulations of AT9283 exposure at the MTD in (a) adults with solid tumours, (b) adults with leukaemia, (c) children with solid tumors, (d) and the estimated MTD in children with leukaemia (500 mg/72h). The black solid lines are the median AT9283 concentrations and the shaded areas are the 90% prediction intervals of the simulations.

Figure 4. Simulated median AT9283 concentrations at a dose of 30/kg/72 h over a range of GFR and weight. *GFR* glomerular filtration rate, *WGT* body weight.

Figures

Figure Legends

Figure 1. Goodness-of-fit plots of the final model. The open circles are the observations from the adult dataset and the open triangles are the observations from the children. The population prediction and individual prediction plots are shown with the line of identity (black) and a linear regression line (blue). Plots of CWRES are shown with a loess smooth (blue line). *CWRES*, conditional weighted residuals.

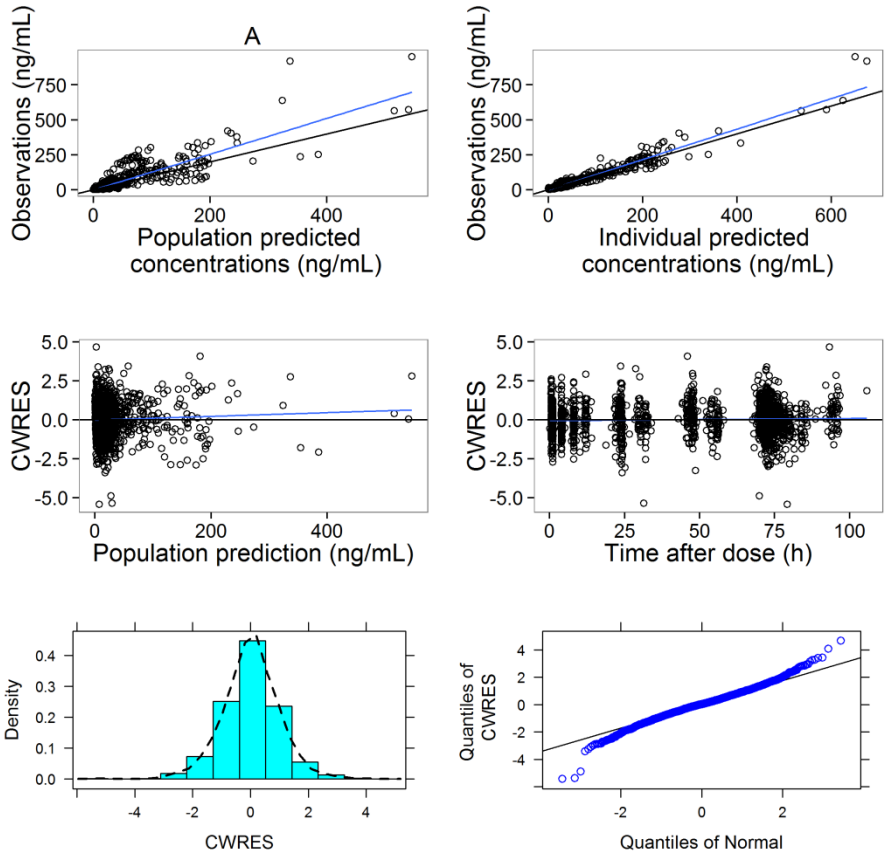

Figure 2. Prediction-corrected visual predictive checks (VPCs) of the AT9283 concentrations stratified by population. The dots are the observations plotted with the median observed AT9283 concentrations (red line) and the 5th and 95th percentiles of the observed concentrations (dotted blue lines). The shaded areas are the 95% confidence intervals of the 5th, 50th and 95th percentiles of the simulated concentrations.

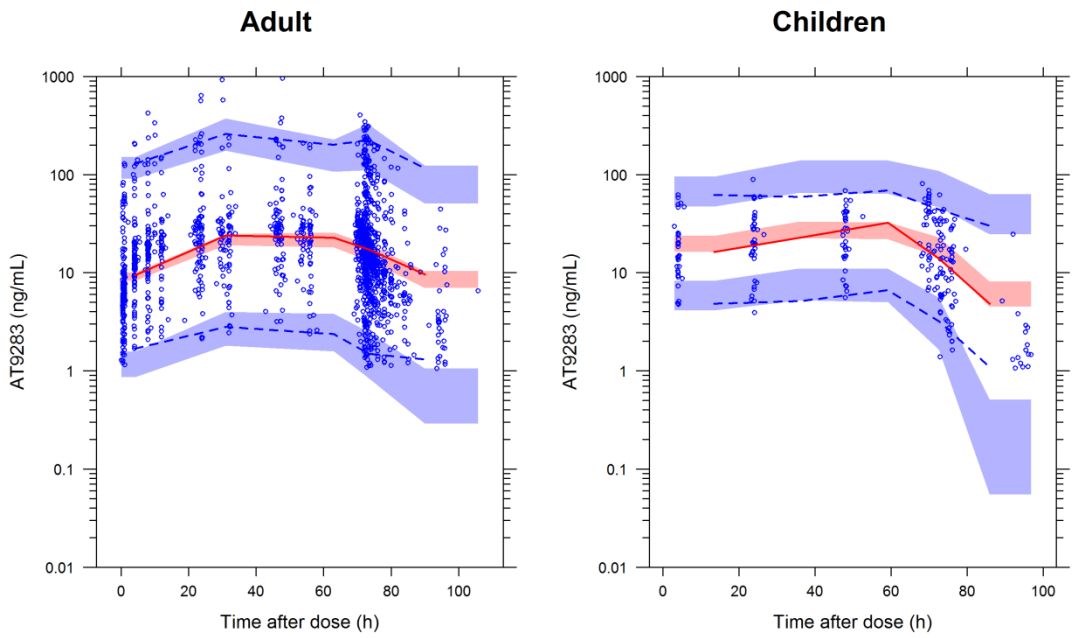

Figure 3. Simulations of AT9283 exposure at the MTD in (a) adults with solid tumours, (b) adults with leukaemia, (c) children with solid tumors, (d) and the estimated MTD in children with leukaemia (500 mg/72h). The black solid lines are the median AT9283 concentrations and the shaded areas are the 90% prediction intervals of the simulations.

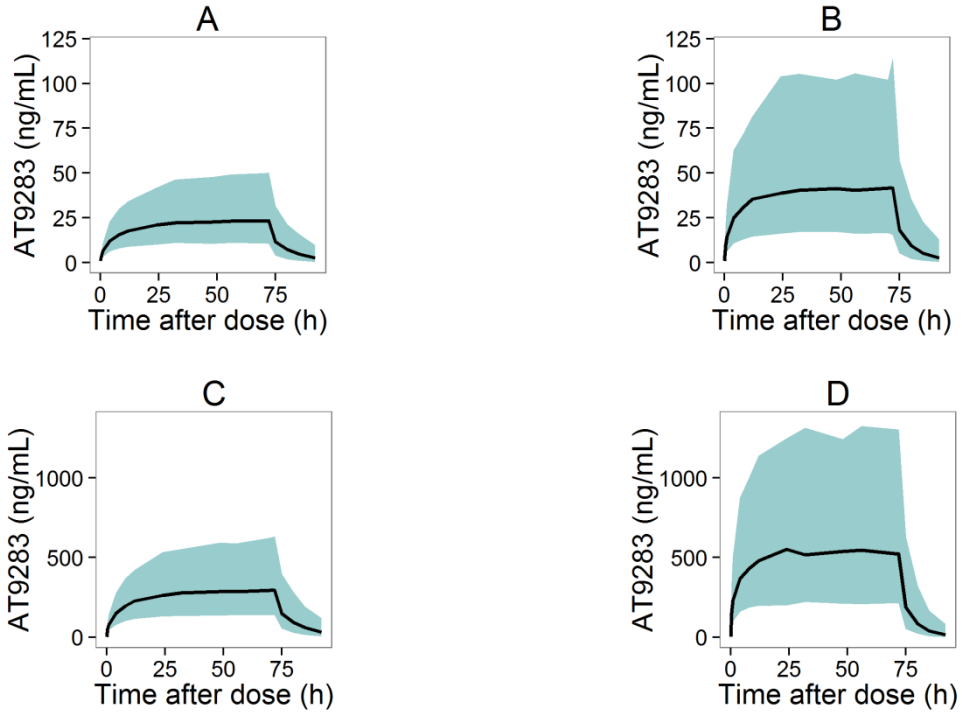

Figure 4. Simulated median AT9283 concentrations at a dose of 30/kg/72 h over a range of GFR and weight. *GFR* glomerular filtration rate, *WGT* body weight.

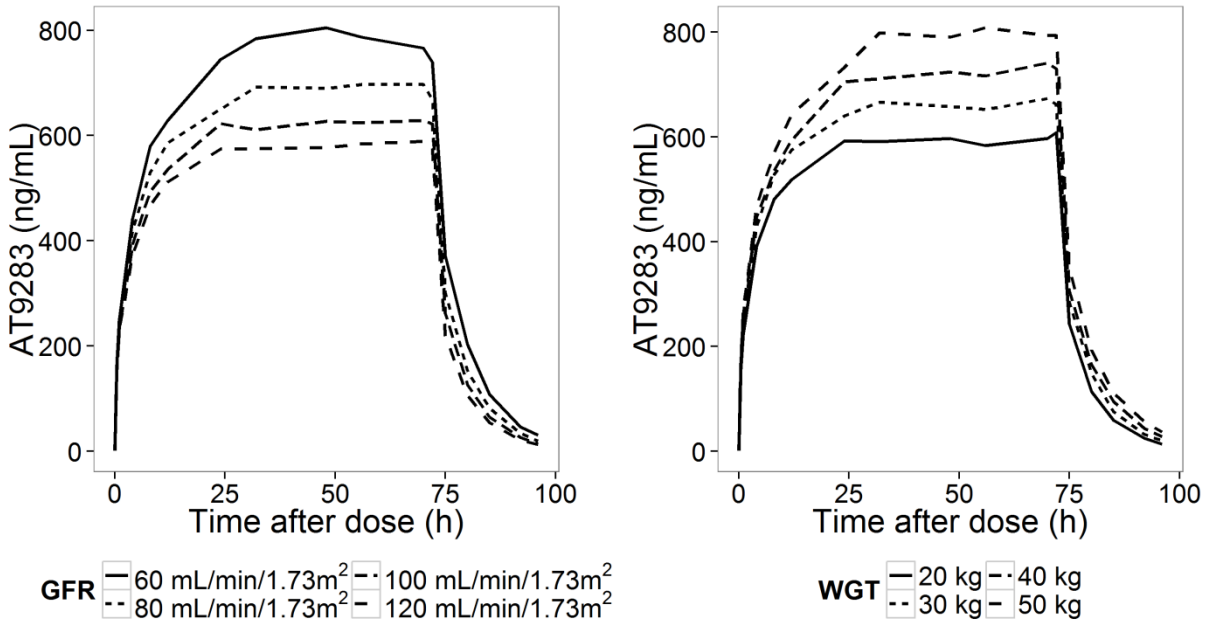

Table 1. The study design of Phase I clinical trials of AT9283.

Study	Arkenau et al. 2012	Foran et al. 2014	Moreno et al. 2015	Cancer Research UK
Trial Identifier	NCT00443976	NCT00522990	NCT00985868	NCT00522990
Population	Adults	Adults	Children	Children (6 months to 18 years)
Cancer	Solid tumors	Relapsed or refractory leukaemias	Solid tumors	Relapsed or refractory acute leukaemias
Recruitment period	2006 – 2009	2006 – 2009	2009 - 2012	2011 - 2014
Study Design	3+3	3+3	Rolling six	3+3
Doses ($mg/m^2/72h$)	4.5 to 36	9 to 486	21– 66	27– 69
Blood time-points (h after dose)	0.5, 1, 4, 8, 12, 22, 32, 46, 56, 70, 72, 72.05, 72.25, 72.30, 72.45, 73, 74, 75, 76, 78, 80, 84, 96 h and day 8 in cycles 1 and 2.	0.5, 1, 4, 8, 12, 22, 32, 46, 56, 70, 72, 72.05, 72.25, 72.30, 72.45, 73, 74, 75, 76, 78, 80, 84, 96 h and day 8 in cycles 1 and 2.	0, 4, 24, 48, 70, 73, 76 and 96 h after the start of the infusion cycle 1.	0, 4, 24, 48, 70, 73, 76 and 96 h after the start of the infusion cycle 1.
Identified MTD ($mg/m^2/72h$)	27	324	55.5	-

Table 2. Demographics of subjects enrolled in Phase I trials. Values are median (range).

	Astex Pharmaceuticals		Cancer Research UK	
Population	Adults		Children	
Cancer	Solid tumour	Leukaemia	Solid tumour	Leukaemia
N	29	24	32	7
Dose (mg/m^2/72 h)	27 (4.5 – 36)	36 (9 – 486)	39 (21 – 69)	43.5 (27 – 69)
Age (y)	63 (34 – 77)	54 (22 – 86)	9 (3 – 18)	3 (1 – 18)
Weight (kg)	73.6 (48.7 – 120.5)	67.4 (41.9 – 114)	29.2 (12.6 – 62.5)	16.1 (8.9 – 59.7)
BSA (m^2)	1.80 (1.50 – 2.50)	1.78 (1.32 – 2.41)	1.02 (0.56 – 1.69)	0.68 (0.44 – 1.70)
BMI (kg/m^2)	25.1 (14.9 – 34.9)	23.9 (17.2 – 43.6)	17.0 (14.1 – 24.1)	16.8 (13.2 – 21.2)
GFR (mL/min/1.73 m^2)	76.5 (51.4 – 125.7)	78.9 (31.9 – 170.5)	125.5 (47.4 – 229.2)	154.3 (129.6 – 299.4)

Table 3. Final population parameter estimates from the final model. IIV, inter-individual variability (%), RSE, residual standard error.

	Parameter estimate (RSE%)	**Bootstrap results Median (range)**
CL (L/h/70kg)	32.3 (5)	32.2 (30.0 – 34.9)
V_C (L/70kg)	58.6 (7)	58.5 (50.1 – 64.9)
Q (L/h/70kg)	38.5 (12)	39.2 (32.5 – 49.2)
V_P (L/70kg)	162 (6)	162 (148.3 – 179.5)
GFR exponent	0.453 (23)	0.452 (0.206 – 0.606)
IIV (%)		
η_{CL}	42.9 (9)	43.1 (36.2 – 49.6)
η_{VC}	29.8 (17)	30.5 (22.0 – 40.8)
η_{Q}	77 (18)	74.1 (44.5 – 98.7)
η_{VP}	38.9 (13)	38.6 (30.4 – 47.7)
Residual errors		
Adults		
Additive (ng/mL)	0.166 (6)	0.163 (0.145 – 0.181)
Proportional (%)	49.9 (24)	50.0 (28.1 – 75.8)
Children		
Additive (ng/mL)	0.359 (8)	0.359 (0.308 – 0.409)

Table 4. Model-derived AUC for each group at the MTD. Values are median (range).

	Adults with solid tumors	Adults with leukaemia	Children with solid tumors	Children with leukaemia
BSA (m^2)	1.9	1.75	1.22	0.74
GFR (mL/min/1.73m^2)	79	77	117	154
MTD dose (mg/72h)	51.3	567	67.7	500*
AUC (h.ng/mL)	1653 (364 – 6307)	20,956 (4774 – 76,805)	2984 (681 – 14220)	38,254 (9694 – 124,430)

*Simulated MTD for children with leukaemia.

Supplementary Figure 1. The distribution of GFR in adults and children. *GFR*, glomerular filtration rate.

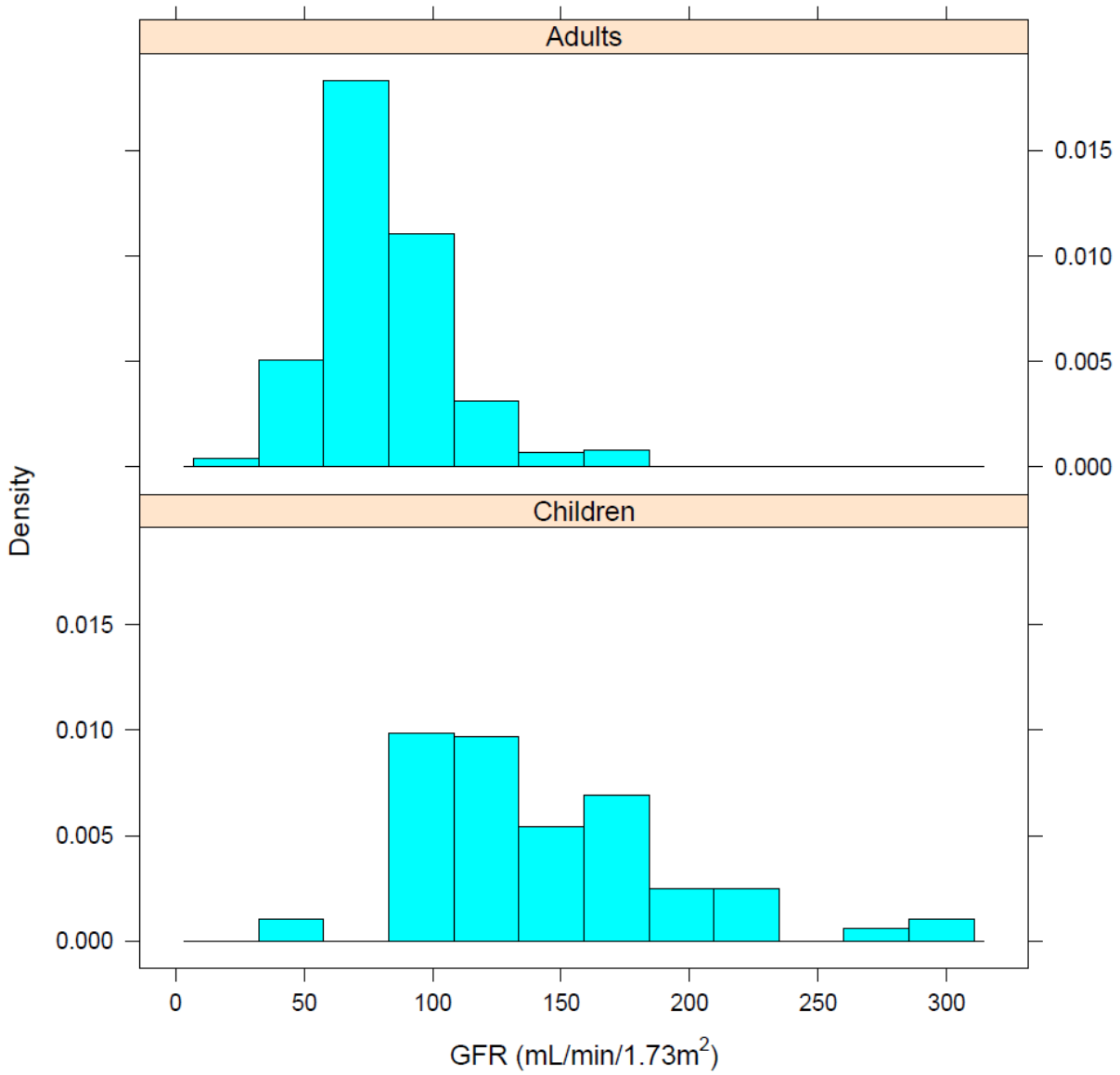

Supplementary Figure 2. The simulated distribution of AUC at the maximum tolerated dose. For children with leukaemia, a dose of 500 mg/72h was used for the simulations. *AUC*, area under the curve.

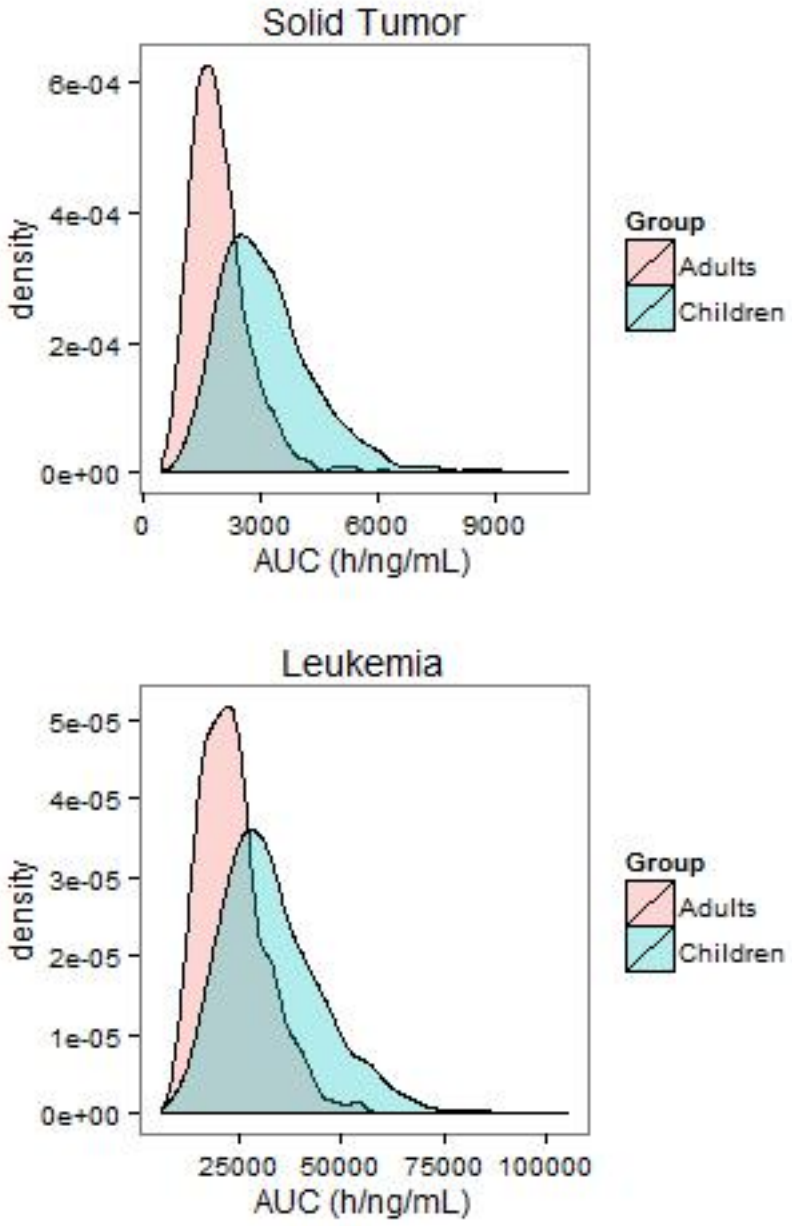

Supplementary Figure 3. The observed concentrations plotted against population predicted concentrations and individual predicted concentrations, stratified by weight.

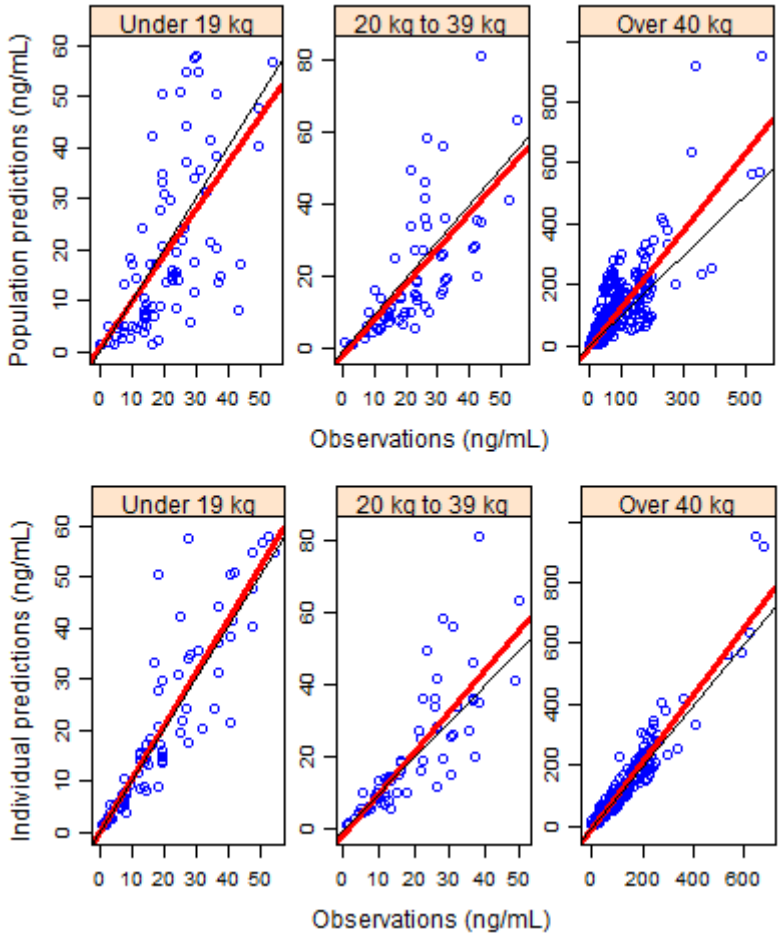

Supplementary Figure 4. Model-derived AUC for flat dosing of 500 mg/72 h vs weight-based dosing of 30 mg/kg/72 for children at varying weights

.